MADRID
inter.noise 2019
June 16 - 19
NOISE CONTROL FOR A BETTER ENVIRONMENT

A study on the application of locally resonant acoustic metamaterial for reducing a vehicle's engine noise

Chang, Kyoung-Jin[1]
Sound Design R/Lab, Hyundai Motor Company
150, Hyundaiyeonguso-ro, Namyang-eup, Hwaseong-si, Gyeonggi-do, South Korea

Rocha de Melo Filho, Noé Geraldo[2]
KU Leuven, Dept. of Mechanical Engineering and DMMS Lab, Flanders Make
Celestijnenlaan 300, B-3001 Heverlee, Belgium

Van Belle, Lucas[3]
KU Leuven, Dept. of Mechanical Engineering and DMMS Lab, Flanders Make
Celestijnenlaan 300, B-3001 Heverlee, Belgium

Claeys, Claus[4]
KU Leuven, Dept. of Mechanical Engineering and DMMS Lab, Flanders Make
Celestijnenlaan 300, B-3001 Heverlee, Belgium

Desmet, Wim[5]
KU Leuven, Dept. of Mechanical Engineering and DMMS Lab, Flanders Make
Celestijnenlaan 300, B-3001 Heverlee, Belgium

ABSTRACT

In automotive development satisfying both low noise and lightweight is challenging since most of the conventional noise and vibration countermeasures such as insulation pad, deadener and reinforcing material have their performance closely related to their mass. This paper proposes a novel noise and vibration insulation pad design based on locally resonant metamaterial to improve the noise and vibration insulation of a vehicle while reducing the weight of the current sound insulation pad. In the first part, a major automotive noise issue due to the engine noise is introduced, and various resonant metamaterial designs are devised and their noise and vibration insulation performance is experimentally assessed. In the second part, the selected resonant metamaterial designs are applied to a firewall panel in a real car. Their noise insulation performance is again experimentally evaluated. As a result, the insulation pad with resonant metamaterials is lighter and acoustically outperforms the current insulation pad solution in the frequency

[1] changkj@hyundai.com
[2] noegeraldo.rochademelofilho@kuleuven.be
[3] lucas.vanbelle@kuleuven.be
[4] claus.claeys@kuleuven.be
[5] wim.desmet@kuleuven.be

region where the resonant metamaterials are effective while having similar acoustical performance outside this frequency region.

Keywords: resonant metamaterial, firewall, engine noise
I-INCE Classification of Subject Number: 33

1. INTRODUCTION

Noise and vibration countermeasures such as insulation pad, deadener and reinforcing material are commonly used to improve engine noise radiated from the firewall of a vehicle. These countermeasures bring about weight increase of a vehicle since their performance is generally related to their mass. Nevertheless, lightweight design is an increasingly requirement due to the ecological trend [1]. Consequently, automotive development has the challenge to deliver cars with high noise and vibration harshness (NVH) comfort while maintaining the lightweight design. Recently, resonant metamaterials have emerged as a potential lightweight NVH solution [2]. They can offer superior NVH performance in specific and tunable frequency ranges, referred as stop bands. These stop bands are induced due to a Fano-type interference generated by the addition of resonant structures in a host structure in a subwavelength scale [3]. The theory and potential of a locally resonant metamaterials have been discussed in many works [4-8]. In this paper, three resonant metamaterial designs are devised to improve the NVH performance of a vehicle while reducing the weight of the current sound insulation pad, which is mounted on its firewall. The NVH performances of these designs are experimentally assessed and compared with the current insulation pad solution in a lab test rig. From this test, two resonant metamaterial designs are selected and added to a firewall of a passenger car to experimentally verify the noise insulation performance. In conclusion, the designed metamaterial solutions are lighter and surpass the NVH performance of the current insulation pad in the tuned stop band.

2. AUTOMOTIVE NOISE ISSUES

2.1 Noise Measurement of a Passenger Car

In order to decide the target frequency of the stop band, the SPL of a diesel engine car has been measured in three positions, i.e. the right side of a driver seat headrest, the front of a left dash panel and at the rear of the engine block in the engine compartment, respectively in idle and drive condition (Figure 1).

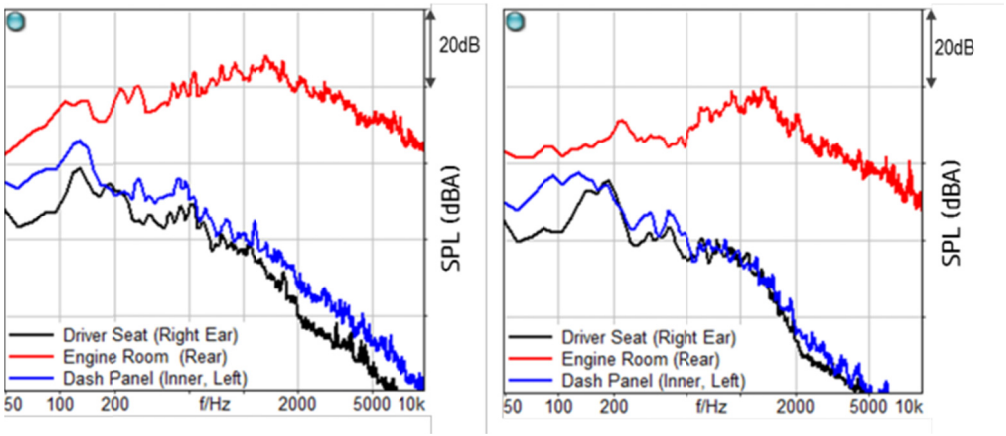

Figure 1: SPL measurement of a diesel engine car: idle (left) and drive condition (right)

In Figure 1, the highest SPL peak in the engine room is considered the frequency range in which the combustion noise is the loudest, i.e. 1100 – 1500 Hz. Therefore, the 1st target for the stop band is set for this frequency range.

Also, the potential of having two stop bands in one resonant metamaterial treatment is exploited, which means the first target is maintained, and a second target is defined to a frequency region from 700 – 1100 Hz. Later this second target is shifted to 400 – 700 Hz due to a measured peak in structural vibrations on the firewall, which is shown later in this paper.

2.2 Test Samples and Test Condition

Engine noise transmission through the dash panel into the car cabin is one of the main NVH issues in a vehicle. To enhance the transmission loss, it is necessary to add a dash insulation pad on the firewall as seen in Figure 2. It usually consists of a sound insulation layer, e.g. ethylene-vinyl acetate (EVA) sheet or ammonium perchlorate (AP) coated sheet, and a sound absorption layer, e.g. polyurethane (PU) foam or polyethylene terephthalate (PET) fibre. These two layers complement each other to improve the sound transmission loss in the low and high frequency. However, the sound insulation pad has its performance closely related to its mass, which poses a constraint in achieving high levels of NVH comfort.

Figure 2: Firewall without insulation pad (left) and the firewall with the dash insulation pad installed (right).

In this study, an original dash insulation pad which is composed of three layers, i.e. PET fibre, 2.5mm thickness EVA and PU foam is compared with the resonant metamaterial dash insulation pad having four layers, i.e. PET fibre, 1.0 mm thickness EVA, PU foam and a resonant metamaterial layer. The resonant metamaterial sample is glued to a host structure, herein a flat steel panel, with instant adhesive (Figure 3), and the other layers are attached to the host structure using bolts. In the real vehicle test, a fire wall corresponds to the host structure.

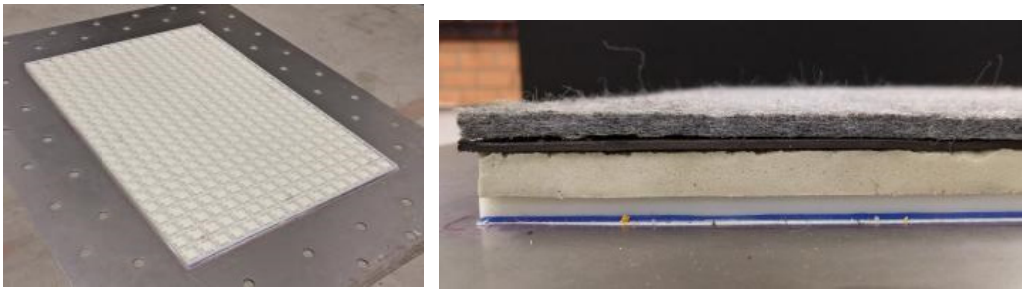

Figure 3: Metamaterial layer added to a steel panel (left) and metamaterial insulation pad composition (right) from top to bottom: PET fibre, EVA, PU foam and metamaterial layer.

The noise insulation performances of the metamaterial treatments are first evaluated by insertion loss (IL) measurements in the KU Leuven Soundbox [9] (Figure 4). The Soundbox is made of reinforced concrete and has a 35 mm thick aluminum front wall where the sample to be tested is clamped on an A2 (420 x 594 mm) size aperture by 52 bolts, where a 30 Nm torque is applied on each bolt. In this way, the samples of dash insulation pad with an A2 size are tested. These samples are tested together with a flat 1 mm thickness steel plate, which represents the firewall, and it has the same acoustic wetted surface area of the insulation pad, (Figure 3). The IL is calculated as:

$$IL(f) = 10\log_{10}\frac{W_{open}}{W_{closed}}, \tag{1}$$

where W_{open} and W_{closed} are the measured sound power of the cavity open and closed by the test sample, respectively, when excited by a loudspeaker inside the cavity. The sound power is measured using a B&K PP probe type 2681 with a spacer of 12 mm. The temperature inside the Soundbox during the measurements was of 20ºC.

The structural vibration behaviour of the steel plate clamped to the cavity with the dash insulation pads installed is also measured by impact testing over a regular grid of 7x8 points on the A2 size acoustic wetted surface. A hammer with impedance head type PCB 086C03 and an accelerometer type PCB 35A24, weighing 0.8 g are used as excitation and response measurement respectively.

Figure 4: IL is calculated with the sound power radiated in the KU Leuven Soundbox open (left) and closed by the test sample (right) when excited by a loudspeaker.

The tests in the vehicle are done by exciting the engine room with a loudspeaker (Figure 17) and measuring the SPL at the right side of the driver seat headrest using a microphone PCB 378B20. During the tests the instrumented panel module is not installed as shown in Figure 2. The temperature during the tests inside the car cabin was of 25ºC.

3. CASE STUDIES OF METAMATERIAL DESIGN

In this section, three types of resonant metamaterials are designed and tested in the Soundbox. For each type, finite element based unit cell modelling in combination with the Bloch-Floquet boundary conditions is used to derive

dispersion diagrams, which are used to predict the stop bands [10-12]. Based on this design tool, the stop bands are tuned to the target frequency regions.

3.1 Design and Test of Sample 1A

By reducing the thickness of the EVA from 2.5mm to 1.0mm, 700g has been saved in the A2 size of dash insulation pad. Instead, 612g of resonant metamaterial structure is added, which consists of 368 unit cells (Figure 5). The stop band is created by the first out-of-plane mode of the resonator (Figure 5) in the acoustically relevant bending waves of the steel plate which acts as host structure for the resonators. The stop band is identified by the frequency wave gap from 1549 Hz to 1639 Hz in the obtained dispersion diagram (Figure 6), which is calculated along an irreducible Brillouin contour also shown in Figure 6. The designed metamaterial is then realized by stereo-lithography using ProtoGen white as the material (Figure 7).

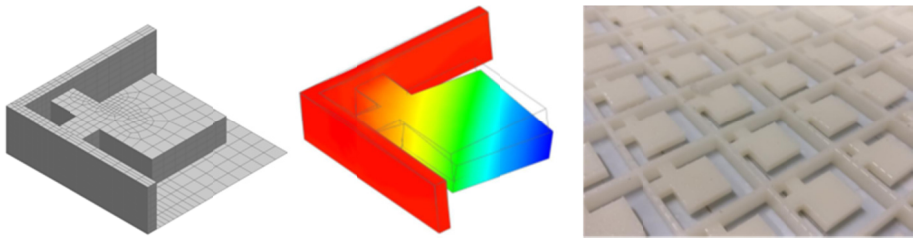

Figure 5: Unit cell (left), first out-of-plane resonator mode responsible for the stop band creation (centre) and resonator array (right)

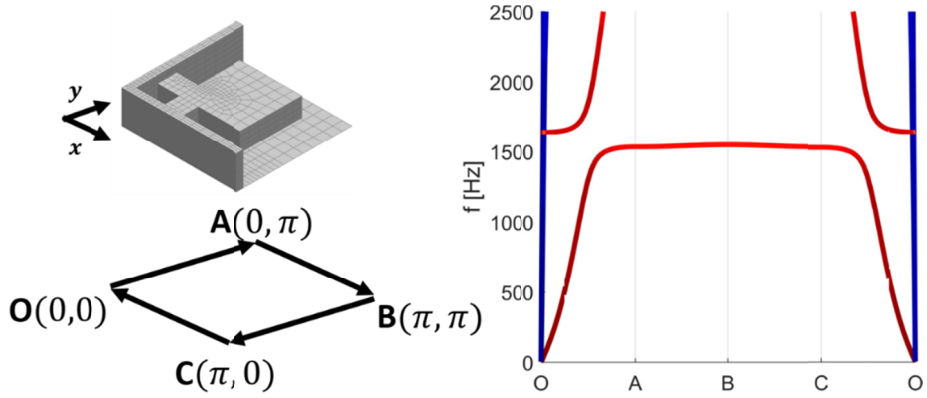

Figure 6: Brillouin contour (left) used to obtain the dispersion diagram (right), where the stop band can be noticed in the targeted acoustically relevant bending waves (red lines), the blue lines represents the in-plane waves.

Three cases are experimentally evaluated. Original case composed of 1 mm thick steel panel and insulation pad with 2.5 mm thick EVA. Sample 1A composed of 1 mm thick steel panel, resonant metamaterial 1A layer (Figure 7) and insulation pad with 1.0 mm thick EVA and a dummy sample composed of 1 mm thick steel panel, a dummy polymethyl methacrylate (PMMA) grid without resonant structures (Figure 7) and insulation pad with 1.0 mm thick EVA. The dummy sample mimics the spacing created between steel panel and insulation pad by the resonant metamaterial layer, however, it does not create stop band effect.

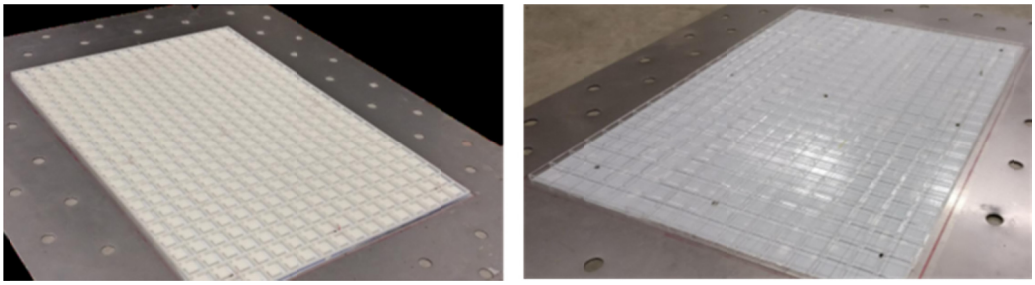

Figure 7: Sample 1A (left) and dummy sample (right) on which sound insulation pads are added for measuring the vibration behaviour and IL.

Figure 8 shows that the metamaterial sample 1A presents overall lower vibrations levels than the other two cases, even though it is 7.6 % lighter than the original sample. Moreover, the sample 1A shows the pronounced vibration attenuation in the frequency region of the predicted stop band.

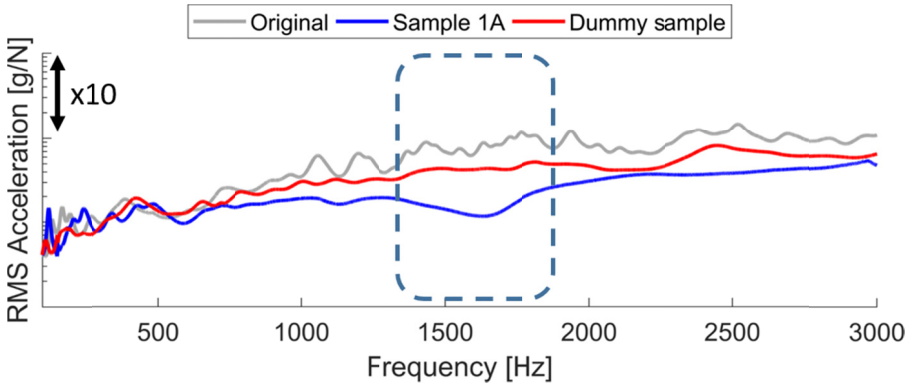

Figure 8: FRF of the RMS acceleration calculated over the points of the defined regular grid for the original, sample 1A and dummy sample cases. The dashed rounded rectangle highlights the stop band effect.

In the IL results (Figure 9), the resonant metamaterial sample 1A outperforms the original sample for frequencies above 500 Hz and has similar performance for frequencies below. The sample 1A also has similar performance to the dummy sample throughout the analyzed frequency range, except in the frequency region of the stop band where the former outperform the latter due to the stop band effect.

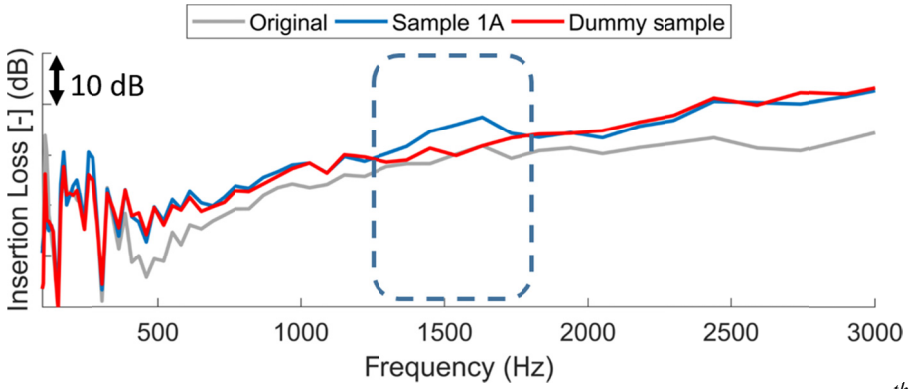

Figure 9: IL of the three cases original, sample 1A and dummy sample in 12th octave bands. The dashed rounded rectangle highlights the stop band effect.

3.2 Design and Test of Sample 3A

In order to minimize the weight of the resonant metamaterial layer while keeping its performance, the unit cell has been redesigned as shown in Figure 10. The stop band is predicted from 1246 Hz to 1268 Hz, in the same manner as for the sample 1A. The sample 3A consists of 204 unit cells with an insulation pad with 1 mm thick EVA (Figure 11).

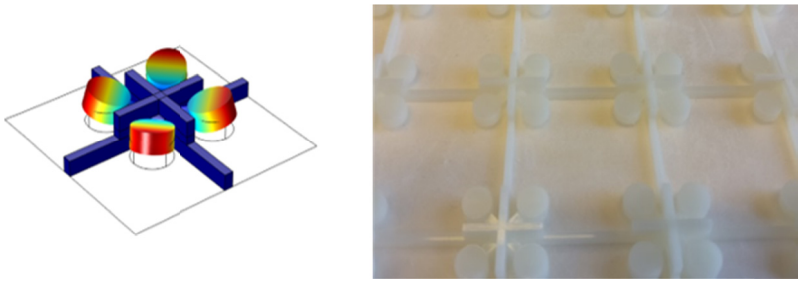

Figure 10: Unit cell of sample 3A showing the out-of-plane mode of the resonator (left) and its realization (right).

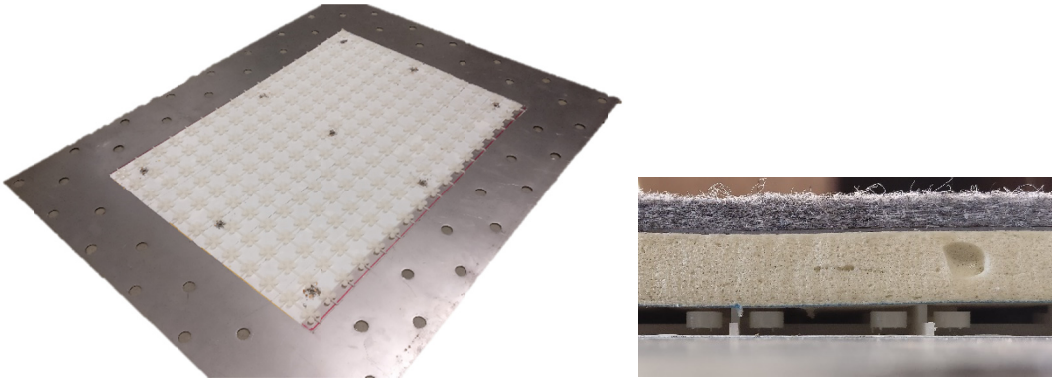

Figure 11: Sample 3A installed in 1 mm steel panel (left) and side view with the insulation pad installed on top (right).

The measured structural vibration behaviour and IL show that the stop band effect exists in the predicted frequency region. Nevertheless, the stop band effect is less pronounced for this metamaterial case. This is caused by the lower weight of the added resonators in sample 3A, 214 g, which represents a weight reduction of 41.9% from the total weight of the 2.5 mm EVA.

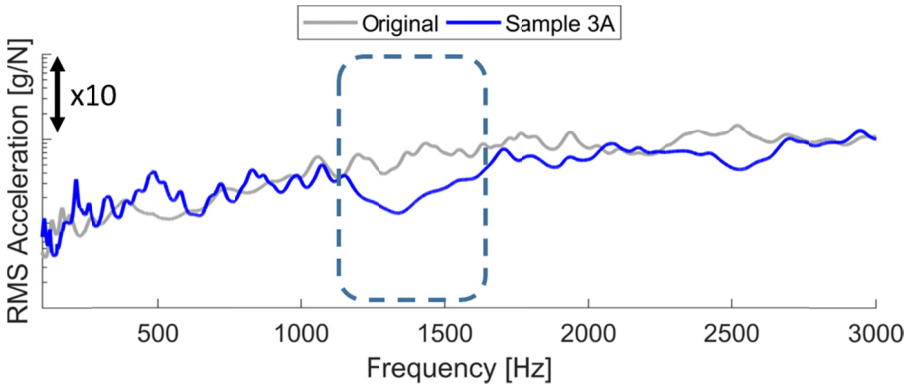

Figure 12: FRF of the RMS acceleration calculated over the points of the defined regular grid for the original and sample 3A cases. The dashed rounded rectangle highlights the stop band effect.

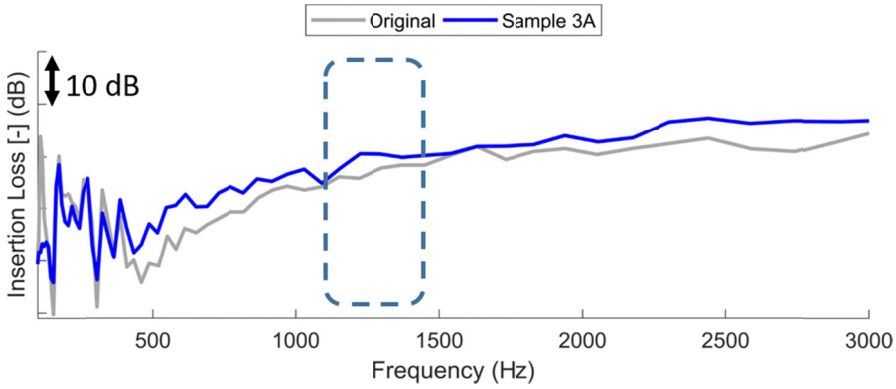

Figure 13: IL of the cases original and sample 3A in 12th octave bands. The dashed rounded rectangle highlights the stop band effect.

3.3 Design and Test of Sample 4A

In order to widen the stop band effect, the design of sample 3A has been modified as shown in Figure 14, where each unit cell has two pairs of resonators with different tuned frequencies, so that it can exhibit two different stop bands, which are predicted from 899 Hz to 913 Hz and 1246 Hz to 1276 Hz.

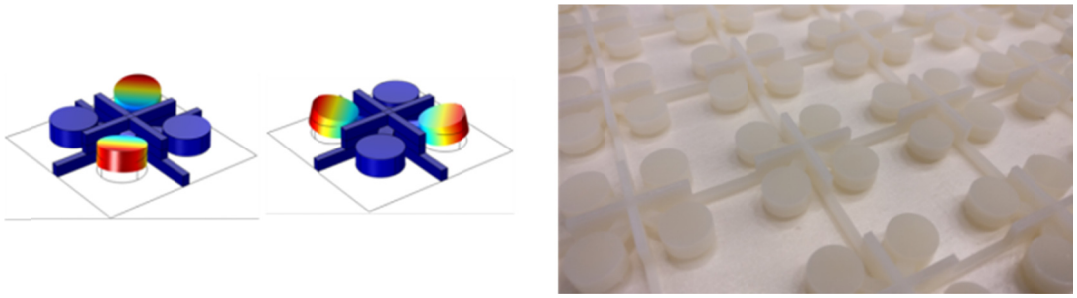

Figure 14: Unit cell of sample 4A and the two out-of-plane modes of the resonator (left) and its realization (right).

Figure 15 and Figure 16 show that this sample clearly presents lower levels of vibration and higher IL than the original insulation pad in the two frequency ranges of the predicted stop bands. The total weight of this sample 4A is 420g and thus the weight reduction is of 24.1% of the total weight of the 2.5 mm EVA. This type of resonant metamaterial can be an alternative measure when a separate or broadband stop band is necessary, although the performance and weight reduction may be somewhat sacrificed.

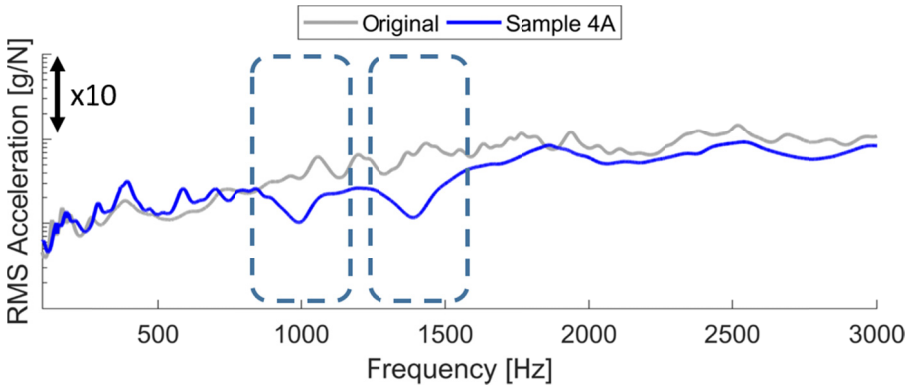

Figure 15: FRF of the RMS acceleration calculated over the points of the defined regular grid for the original and sample 4A cases. The dashed rounded rectangles highlight the stop bands effect.

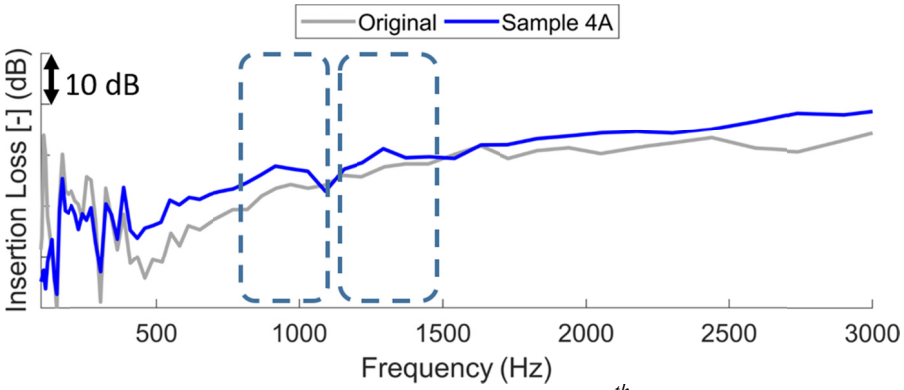

Figure 16: IL of the cases original and sample 4A in 12th octave bands. The dashed rounded rectangles highlight the stop band effect.

4. VEHICLE TEST

4.1 Pre-test for Identifying the Position of AMM Structure

To verify the performance in vehicle, two of the presented resonant metamaterial samples are applied to a firewall of a diesel engine powered passenger car. The resonant metamaterial samples are aimed to cover an area below 50% of the firewall to maximize the performance with a small weight.

A vibro-acoustic modal test has been performed in advance to identify the zones of highest vibrations amplitude and confirm the target frequencies. In this way, the vibration level at 1308 points of the firewall were measured by a laser vibrometer (Polytec PSV-500) during acoustic excitation in the engine room provided by a loudspeaker as seen in Figure 17. The RMS velocity of the measured points shows that there exists a dominant peak due to the bending mode of the firewall around 568Hz and a few unpronounced peaks around 1000Hz (Figure 17). Therefore, the second stop band frequency range target is chosen to be 400 – 700 Hz, while the first target is maintained.

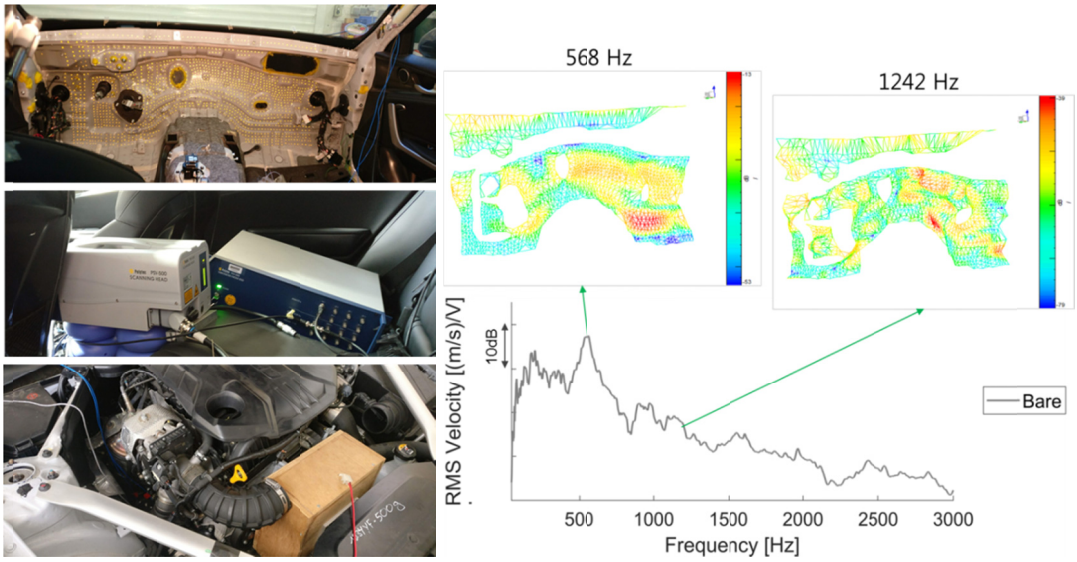

Figure 17: Vibro-acoustic modal test setup (left) and vibration pattern at two-targeted frequencies together with the calculated RMS velocity in 1308 measured points (right).

The analysis of the vibration pattern at this two frequency ranges shows that the vibrations at 400 – 700 Hz are mainly concentrated on the firewall right side while

the vibrations at 1100 – 1500 Hz are concentrated on middle of the right side of the firewall and in its lower left side (Figure 17). These places were defined as the zones to be treated with resonant metamaterial samples (Figure 18). For the final selection of the places to add resonators, also the availability of flat surfaces in the selected areas was taking into account.

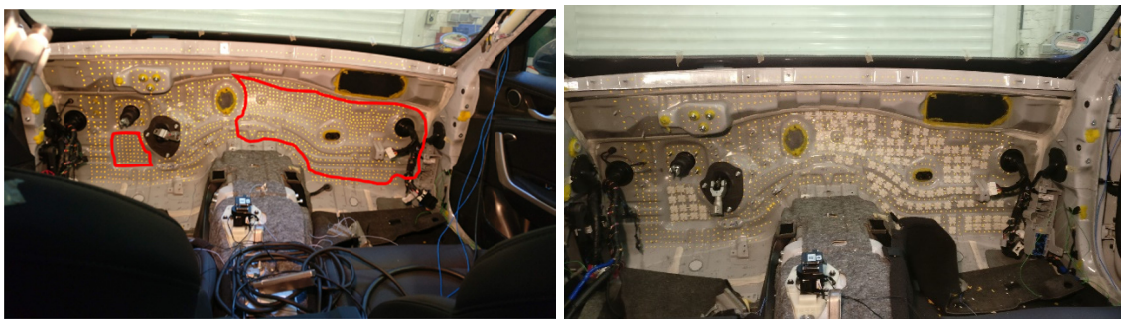

Figure 18: Identified zones to be treated are marked in red (left) and firewall treated with resonant metamaterial sample 3B (right).

4.2 Design and Test of Sample 3B

Since only 50% of the area is covered with resonators, a detailed size has been updated on the design of Sample 3A such that more mass can be used in the resonator, without changing the targeted zone of reduction. The new design leads to weight addition of 318 g and a stop band from 1258 to 1365 Hz. For the tests, the firewall is treated with 140 unit cells of sample 3B, which are glued with an instant adhesive as shown in Figure 18.

Figure 19 shows the SPL at the right side of a driver seat headrest with two types of insulation pad: the original, which has 2.5 mm thick EVA and the resonant metamaterial with 1.0 mm thick EVA. The resonant metamaterial sample exhibits lower SPL levels than the original sample at the target frequency range without deterioration at the other frequencies. Furthermore, the weight reduction between original and metamaterial insulation pad in the full area of dash isolation pad is of 2401 g, corresponding to 52.4 % of the total weight of the original insulation pad, which is a substantial weight reduction in automotive design.

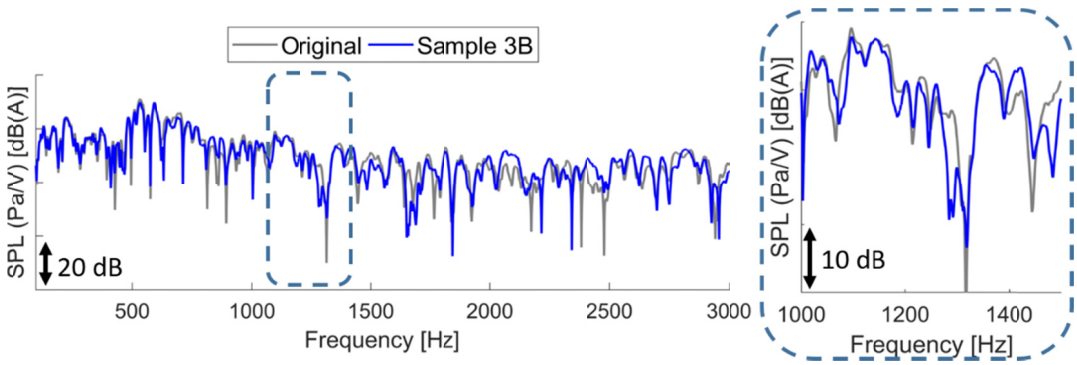

Figure 19: SPL on the right side of the driver seat headrest for the original and sample 3B case. The rounded rectangle shows a zoom in the frequency region of the predicted stop bands.

4.3 Design and Test of Sample 4B

Similar as for sample 3B, sample 4B is an updated version of sample 4A and leads to a stop band from 578-607 and 1294-1352 Hz corresponding with 400 -

700 Hz and 1100 - 1500 Hz as targeted frequency ranges. Similar to Figure 18, 140 unit cells of the sample 4B have been glued on the marked zones. The total weight reduction from the original dash insulation pad for this sample is of 2079 g, corresponding to 52.2 % of the total weight of original EVA. In addition to the great weight reduction, it can be seen that noise transmission is slightly attenuated in the both target frequency regions as shown in Figure 20.

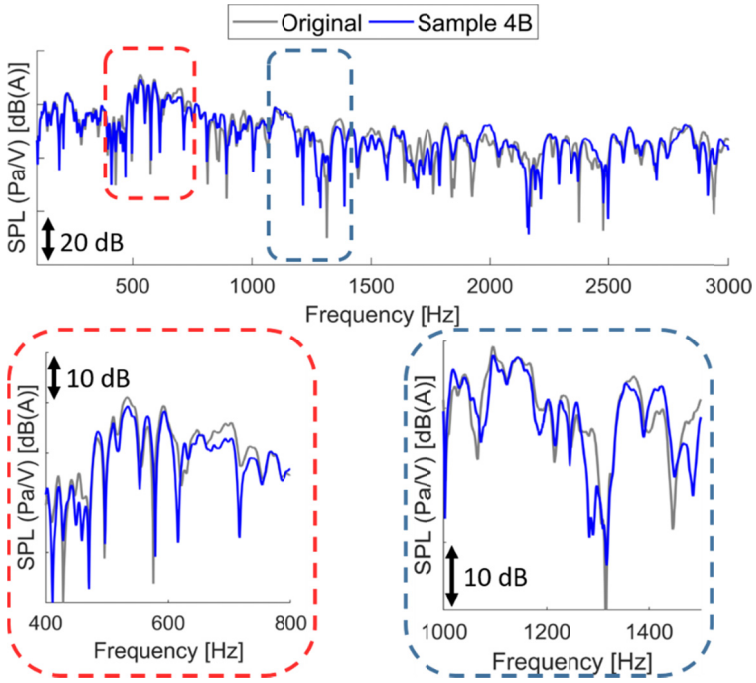

Figure 20. SPL on the right side of a driver seat headrest for the original and sample 3B case. The rounded rectangles show a zoom in the frequency region of the predicted stop bands.

5. CONCLUSIONS

In this study, several kinds of resonant metamaterial designs have been suggested for attenuating the engine noise in the vehicle cabin. For the chosen design, the geometry variables have been calculated to tune the stop band in the target frequencies of engine noise by using unit cell modelling. From the experimental results of structural vibrations and sound insertion loss of the samples obtained in a lab test rig, it is found that the suggested metamaterial samples surpass the NVH performance of the original insulation pad while being lighter. The designs are adapted to be tested on the firewall of a real car, considering NVH performance and mass addition. The weight reduction of the dash insulation pad achieved is of 52 % of the original insulation pad. Moreover, the metamaterial samples show better noise attenuation performance than the original insulation pad at the target frequencies due to the tuned stop band effect without NVH performance deterioration at the other frequencies. Considering the rising needs for weight reduction and noise attenuation, it is expected that such resonant metamaterials can be regarded as a significant countermeasure for the noise and vibration of a vehicle.

6. ACKNOWLEDGMENTS

Most of this research is funded by Hyundai Motor Group. The research of N. F. Melo is funded by a PhD Scholarship Sciences without Borders CNPq Brazil

(201414/2014-7). The research of L. Van Belle is funded by a grant from the Research Foundation - Flanders (F.W.O.). This research was partially supported by Flanders Make, the strategic research centre for the manufacturing industry. Hyundai Motor Group and the Research Fund KU Leuven are gratefully acknowledged for their supports.

7. REFERENCES

1. Mallick, Pankaj K., ed. *Materials, design and manufacturing for lightweight vehicles*. Elsevier, 2010.
2. C. C, Claeys, K. Vergote, P. Sas and W. Desmet, *"On the Potential of Tuned Resonators to Obtain Low-Frequency Vibrational Stop Bands in Periodic Panels"*, J. of Sound and Vibration 332 (2013) 1418-1436.
3. C. Goffaux, J. S´anchez-Dehesa, A.L. Yeyati, P. Lambin, A. Khelif, JO Vasseur, and B. Djafari-Rouhani. *Evidence of fano-like interference phenomena in locally resonant materials*. Physical Review Letters, 88(22):225502, 2002.
4. G. Ma and P. Sheng, *"Acoustic Metamaterials: From Local Resonances to Broad Horizons"*, Science Advances **2**(2), e1501595, DOI: 10.1126/sciadv.1501595.
5. A. O. Krushynska, V. G. Kouznetsova and M. G. D. Geers, *"Towards Optimal Design of Locally Resonant Acoustic Metamaterials"*, J. of the Mechanics and Physics of Solids 71(2014) 179–196.
6. C. C. Claeys, E. Deckers, B. Pluymers, and W. Desmet, *"A lightweight Vibro-Acoustic Metamaterial Demonstrator : Numerical and Experimental Investigation"*, J. of the Mechanical Systems and Signal Processing 70-71 (2016) 853-880.
7. J. Jung, H.-G. Kim, S. Goo, K.-J. Chang and S. Wang, *"Realisation of a Locally Resonant Metamaterial on the Automobile Panel Structure to Reduce Noise Radiation"*, J. of the Mechanical Systems and Signal Processing 122 (2019) 206-231.
8. K.-J. Chang, J. Jung, H.-G. Kim, D. R. Choi, and S. Wang, *"An Application of Acoustic Metamaterial for Reducing Noise Transfer through Car Body Panels"*, SAE Technical Paper 2018-01-1566 (2018), doi:10.4271/2018-01-1566.
9. M. Vivolo. Vibro-acoustic characterization of lightweight panels by using a small cabin. *Diss. PhD Thesis, Arenberg Doctoral School, University of Leuven*, 2013.
10. L. Brillouin, Wave propagation in periodic structures, McGraw-Hill Book Company, 2nd Ed. (1946).
11. B. R. Mace, E. Manconi, Modelling wave propagation in two-dimensional structures using finite element analysis, Journal of Sound and Vibration, Vol. 318, No. 4, (2008), pp. 884–902.
12. F. Maurin, C. Claeys, E. Deckers, W. Desmet, Probability that a band-gap extremum is located on the irreducible brillouin-zone contour for the 17 different plane crystallographic lattices, International Journal of Solids and Structures.